Progress in Superconductivity Vol.1, No.1 pp 20-25 15 August 1999

Construction and Operation of High-T_C Scanning SQUID Microscope

B. Baek[a], Hochul Kim*,[a], Z. G. Khim+,[a], S. -M. Lee[b], S. H. Moon[b], and B. Oh[b]

[a] *Department of Physics, Seoul National University, Seoul 151-742, Korea*

[b] *LG Corporate Institute of Technology, Seoul 137-724, Korea*

Received 5 July 1999

Abstract

We constructed a high-T_C scanning SQUID microscope (SSM) operating in the liquid nitrogen. We used a washer-type YBCO SQUID with inner and outer dimensions of 12 ㎛ and 36 ㎛, respectively, which was grown on the $SrTiO^3$ bicrystal substrate. The sample, rather than SQUID, was scanned using two stepping motors. We also developed readout electronics, stepping motor controller, and the software for system control and data display. We took images of various samples using our SSM and found that the spatial resolution is about 40 ㎛ and noise level is lower than 10^{-7} T/ √Hz at 100 Hz and higher at lower frequencies. The noise level was much higher than that of a typical SQUID due to the other coupling from the electric parts. We present a simple argument on the inductive coupling between the sample and the SQUID which should be understood for the proper interpretation of the obtained images. By comparing the measured data with the simulation results the gap between the SQUID and the sample is estimated to be 40 ㎛.

Keywords: SQUID, scanning SQUID microscope, YBCO, grain-boundary Josephson junction

I. Introduction

The superconducting quantum interference device (SQUID) is the most sensitive magnetic field sensor. Using a SQUID of small size as the sensors of Scanning Probe Microscope,. we can observe the local magnetic field distribution on the sample surface. This is called the Scanning SQUID microscope(SSM). Practical SSM's were first developed in 1983 [1], and have been applied to various research fields including probing of the pairing symmetry in high-T_C superconductors [2], observation of the magnetic domain structures [3], and nondestructive evaluations (NDE) [4].

Since there exist several constraints in making SQUIDs of small size, SSM's spatial resolution is typically several ㎛ at most. Nevertheless, the high magnetic field sensitivity opens various fields of application and has great potentials.

In this paper, we report the construction and operation of the SSM using a high-T_C SQUID [5]. Using high-T_C SQUIDs has the advantages that it enables the operation simpler and makes the cost less compared with a low-T_C SSM. We took magnetic images of several kinds of samples, and present some detailed results about how we can understand the various images. The issues and important points in operating the SSM are also discussed.

II. Construction of SSM

1. SQUID

A $YBa_2Cu_3O_7$(YBCO) film was deposited on a $SrTiO_3$(STO) bicrystal substrate with a misorientation angle of 24° by laser ablation. Four identical SQUID's were designed on a 1 cm × 1 cm substrate,

* Present address : Samsung Electronics, Kyungki-do, Korea

+ Email : jnine@plaza.snu.ac.kr

and cut into 4 pieces after fabrication. The SQUID is washer-type with inner and outer size of 12 ㎛ and 36 ㎛, respectively. One-turn feedback loop was also patterned on-chip just beside the SQUID, whose grain-boundary was shunted with gold in order to avoid the weak link effect. Thin STO film was deposited as a passivation layer to protect the SQUID during the operation.

For scanning, the SQUID chip(7 mm × 1.7 mm) was attached on an epoxy board with printed circuit patterns, then electrical contact leads were made by gold evaporation and silver paste.

2. Electronics

The SQUID was operated with a flux-locked loop(FLL) readout electronics with the flux modulation of 1-10 MHz. We used batteries to drive FLL to reduce noise. The SQUID output signal was fed into the preamplifier through a room temperature transformer. We tried bias reversal technique but got no improvement in the low-frequency noise reduction because the system noise itself is rather high.

The output of the FLL was read by an analog-digital converter (ADC), directly or through a low-pass filter. The bandwidth of the FLL electronics is about 10 kHz. When high frequency signal dominates and the FLL cannot follow abrupt changes of the external signal, the flux-lock can be lost and the operation point jumps to another. In the worst case it leads to the saturation of the electronics and the lock is lost. In this case we must reset the feedback circuit.

The stepping motor control circuit uses PMM8713 which generates high current pulses supplying high torque to the motor. The stepping motors can be operated up to 20,000 pulses per second, but the usual operating condition is about 10,000 pulses per second. For now, this is sufficient considering the bandwidth of the readout electronics and the stability of mechanical parts.

3. Mechanical Parts

Figure 1 shows the schematic drawing of the mechanical part. The SQUID is fixed facing upward, and the sample is attached to the sample block at the bottom of the scanning rod. The SQUID is glued to the copper strip which acts as a spring and ensures soft contact with the sample. The top of the scanning rod was fixed to the two-dimensional translational stage, which is driven by the stepping motors on top of the Dewar. Between the translational stage and the sample block lies a pivot that reduces the motion of the block relative to that of the stage by 1 to 5. One pulse to the stepping motor moves the sample by 0.3 ㎛. It is a reasonable value since the spatial resolution of our SSM is about 40 ㎛.

A Cryoperm can was used to shield external magnetic field. The lower half of the scanning stage is immersed in liquid nitrogen. We used a LHe Dewar with double jackets, and filled both jackets with LN_2. This reduced the boiling rate of the LN_2 in the inner jacket considerably. This results in reduced vibration and longer operation time.

4. Software

Control software is a modified version of the program previously developed in our group to control the scanning tunneling microscope [6]. It controls the stepping motors and acquires data through the 8255

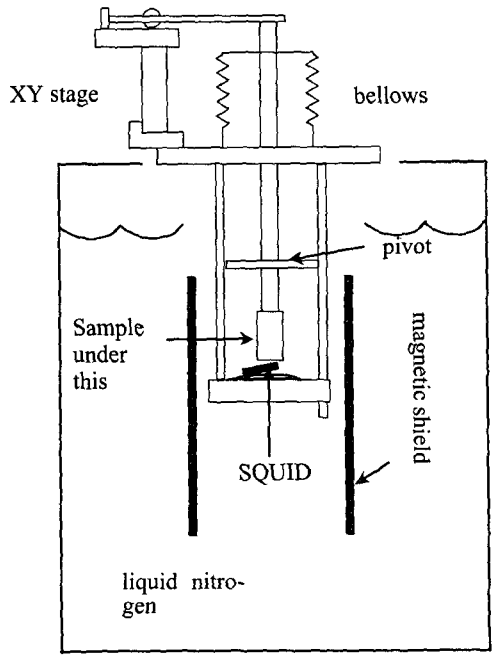

Fig. 1. Design of the scanning SQUD microscope scanning stage.

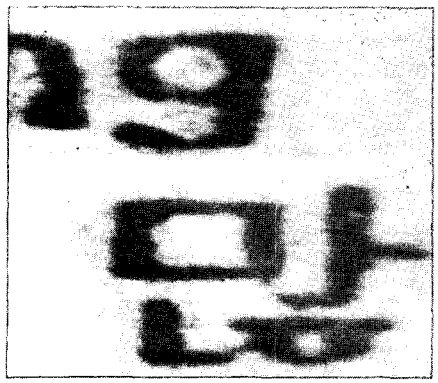

(a)

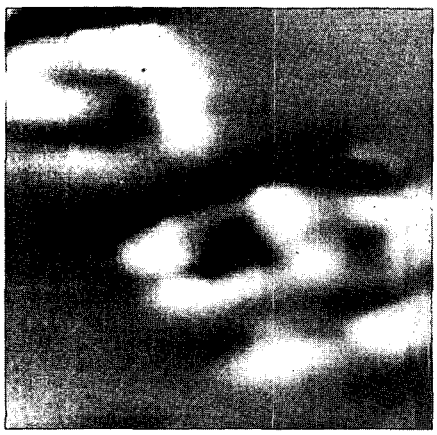

(b)

Fig. 2. (a) Optical image of the laser printer toner pattern (600 dpi.).
(b) SSM image of the toner pattern. The scan area is 2.4 mm × 2.4 mm.

I/O interface card. Scanning is performed line by line to 256 × 256 pixels. During the scanning, first 10 data points of each line were discarded to avoid the effect of hysteresis on the scanned images. An image processing software was used to process the raw data for further detailed analyses, presentation, extraction of line profiles and conversion to other formats.

III. Operations

For each time we operate SSM, we adjusted the SQUID to the optimal operating point by applying magnetic field using an external coil below the sample stage. Bias current, flux modulation frequency, amplitude, relative phase between the modulating signal and the modulated response, and feedback voltage level were adjusted to the stable readout condition of the FLL electronics.

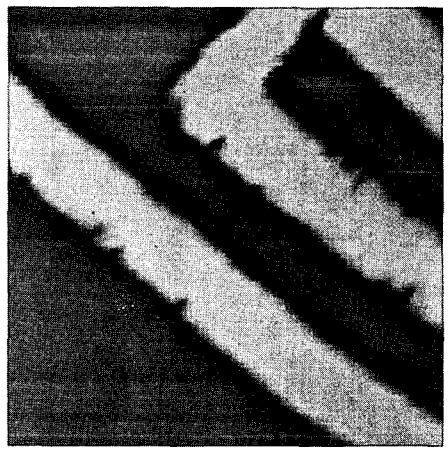

Fig. 3. SSM image of a YBCO meander pattern under external field of about 0.5 gauss. The scan area is 1600 μm × 1600 μm.

The noise level of the total system was measured to be about 10^{-7} T/$\sqrt{\text{Hz}}$ at 100 Hz. The major cause of the relatively high noise level is thought to be the stray capacitive coupling between the stepping motor part and the readout wiring. This high frequency noise caused the FLL operation unstable. By chang ing parts of the mechanical frame from metals to insulating materials, this kind of coupling could be reduced.

As a first demonstration, we got magnetic images of a printed laser printer patterns. Figure 2 shows the optical and SSM images of the printed patterns. Since the printer toner contains ferromagnetic materials, good magnetic image contrast could be obtained by magnetizing it before scanning.

Since superconductor expels magnetic field below the transition temperature (the Meissner effect), it is interesting to probe local magnetic field distribution over a superconducting strip. This local field information is important for both theoretical and application concern.

Figure 3 is the SSM image of YBCO meander pattern at 77 K. Since this sample had been exposed in air for relatively long time, we could observe sev-

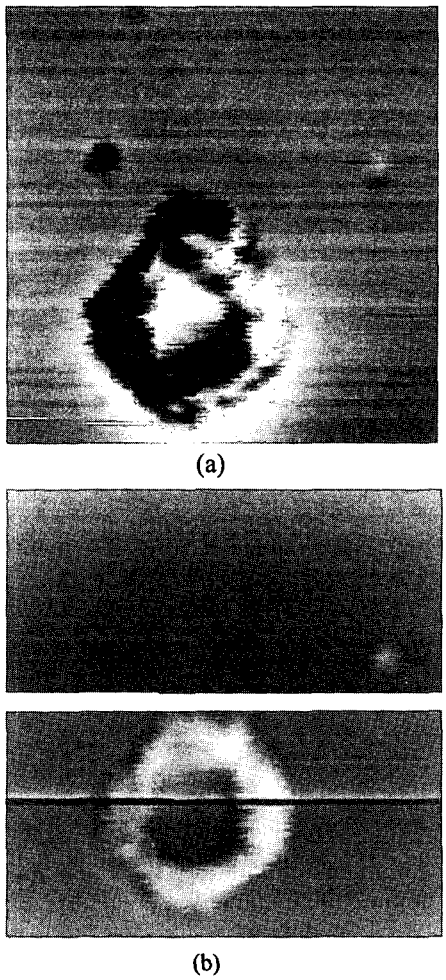

(a)

(b)

Fig. 4. (a) SSM images of a YBCO ring pattern under zero background field. The scan area is 800 ㎛ × 800 ㎛.
(b) The same image as (a) except that the locked flux state has opposite polarity relative to (a). White lines in the middle of the image are due to temporary loss of flux-lock during the scanning.

eral defects on the film and these defects appear in the SSM image. Due to the insufficient spatial resolution of the SSM, we could not distinguish individual flux lines, but only their spatial distribution.

We observed the magnetic field distribution over a ring-shaped YBCO pattern, as shown in Fig. 4. For an SSM image to represent the true magnetic field distribution, the SQUID itself should not affect the sample. However, in the real situation, the nulling field from the feedback coil generates shielding currents in the superconductor sample and causes the mutual inductance between SQUID and the feedback coil to decrease from the real value.

We can see such effects clearly in Fig. 4. Two images were taken under the same operating conditions except for the total magnetic flux threading the SQUID at the locked state. When the SQUID is just over the superconducting strip, the shielding current in the superconductor affect the SQUID and additional feedback current is needed to maintain the SQUID at the locked state. Depending on whether the sign of the total flux in the SQUID is positive or negative, the image of the SQUID in the superconductor strip has different polarity, hence the superconducting strip appears to have different contrast relative to the zero-field background.

Here we will simply consider how the sample-SQUID interaction affects the imaging. When a superconducting slab is scanned with SQUID under zero external magnetic field, the magnetic field generated by the feedback coil cannot penetrate the slab due to the screening. Then the feedback current required to preserve the locked flux state is different from the case without the slab. In the absence of the superconducting slab, the magnetic flux threading the SQUID loop is given by $\Phi = MI$, where M is the mutual inductance between the SQUID and the feedback coil, and I is the feedback current. We can simulate the effect of the superconducting slab by introducing an image coil at the opposite side of the slab, carrying current in the opposite direction. Then the magnetic flux induced by the image coil is given by $\Phi = -\tilde{M}I$, and the total flux is $\Phi_{tot} = (M - \tilde{M})I$. Therefore, we get the expression for the feedback current as $I = \Phi/(M - \tilde{M})$. This means that the feedback current is amplified by $1/(1 - \tilde{M}/M)$ compared with the case without the superconductor, or equivalently, the effective mutual inductance is reduced by that factor.

More generally, if some magnetic field $\Delta\Phi$ is present, e.g., from trapped vortices, the change of the feedback current can be expressed as $\Delta I = -\Delta\Phi/(M - \tilde{M})$. So the total feedback current is given by

$$I + \Delta I = (\Phi - \Delta\Phi)/(M - \tilde{M})$$

Here, we can see that the signal is effectively amplified when the SQUID is over a superconductor, and its contrast depends on the total magnetic flux at the lock state of the SQUID.

The spatial resolution of the SSM depends on the size of the SQUID and the gap between the probe and the sample [2]. The sample-SQUID distance cannot be measured directly, but can be estimated indirectly through simulation.

Figure 5 (a) shows the SSM images of the YBCO wire network. The network is located between the two long pads, but the structure is not seen in this image. To obtain its image, the spatial resolution should have been higher than 20 μm because the unit cell size of the network is 40 μm. The smallest dimension to be seen in the whole image is 40 μm. It is the width of the middle parts of two leads.

We took a line profile of the SSM image of a 80 μm-wide part of the right lead and compared it with a simulation.

For simulation, we assumed infinitely long superconductor strip and perpendicularly applied field, hence converting the problem into the 2-dimensional one. To satisfy the boundary condition of complete exclusion of the magnetic field, screening current distribution was calculated iteratively. Then the magnetic field at any position can be calculated by the current distribution. Obviously, the broadening of the edge profile was observed as the sample-SQUID distance increases. The result is shown in Fig. 5 (b), where symbols are data points and lines are simulation results.

The ratio of the width of the strip to the sample-SQUID gap and the normalization of the magnitude are the fitting parameters. It appears that the simulation result agrees well with the experimental result if we assume the ratio of the width of the strip to the sample-SQUID gap to be 2:1. Considering that the width of the strip is 80 μm, this suggests that the distance between the sample and the SQUID is about 40 μm. This sets the spatial resolution of the SSM to around 40 μm, which are directly confirmed from the scanned images.

To achieve better spatial resolution without losing the high magnetic field sensitivity, field-guiding tip on the SQUID was suggested by some authors [7]. If we implement a soft ferromagnetic tip on the SQUID chip, it will guide magnetic field along the tip surface. Then the higher resolution will be achieved simply by the radius and approach of the tip. We are planning to implement a modified structure of such a flux-focusing tip onto our probe, and theoretical and experimental studies are under way.

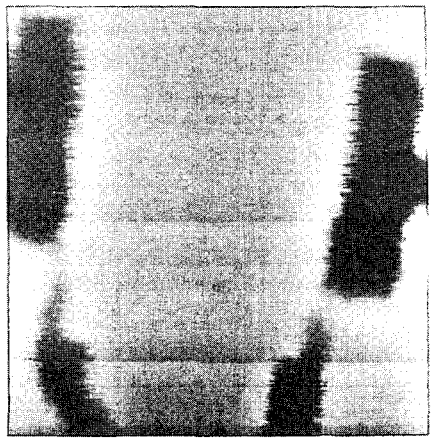

(a)

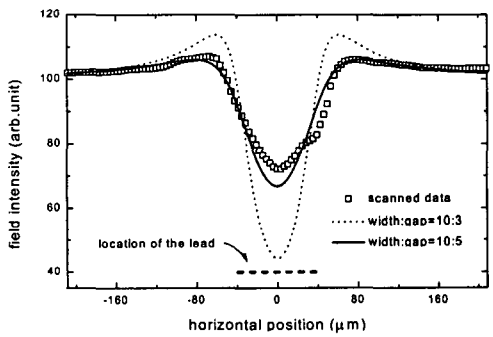

(b)

Fig. 5. (a) SSM image of the YBCO wire network. The scan area is 800 μm × 800 μm.
(b) Line profile of a 80 μm-wide YBCO lead line and computer simulation results.

IV. Conclusion

We have constructed High-T_C scanning SQUID microscope and demonstrated its operation. At the present stage, the spatial resolution is estimated to be around 40 μm and noise level is under 10^{-7} T/$\sqrt{\text{Hz}}$ at

100 Hz. Since this is the first version of SSM, there are a lot to be improved, and much better characteristics are expected. Especially the system noise level is aimed to be that of the SQUID's itself. We expect it to be under 100 pT/ Hz. The couplings between the parts of this system should be eliminated first for noise reduction.

Performing simulations, we could estimate the sample-to-SQUID distance quite reasonably. We also understood how the inductive coupling between the SQUID and the sample and screening by superconducting sample are reflected in the image contrast. These are quite important for correct interpretations of the SSM images.

References

[1] F. P. Rogers, "A Device for Experimental Observation of Flux Vortices Trapped in Superconducting Films", Master Thesis, MIT, Boston, 1983.

[2] J. R. Kirtley, P. Chaudhari, M. B. Ketchen, N. Khare, Shawn-Yu Lin, and T. Shaw, Phys. Rev. B **51**, 12057-12060 (1995).

[3] O. V. Snigirev, K. E. Andreev, A. M. Tishin, S. A. Gudoshnikov, and J. Bohr, Phys. Rev. B **55**, 14429-14433 (1997).

[4] W. G. Jenks, S. S. H. Sadeghi, and J. P. Wikswo Jr., J. Phys. D **30**, 293-323 (1997).

[5] R. C. Black, F. C. Wellstood, E. Dantsker, A. H. Miklich, D. Koelle, F. Ludwig and J. Clarke, IEEE Trans. on Appl. Supercond. **5**, 2137 (1995).

[6] J. H. Lee, Ph. D. Thesis, Seoul National University, 1990.

[7] P. Pitzius, V. Dworak, and U. Hartmann, "Ultrahigh-Resolution Scanning SQUID Microscopy", Ext. Abstr. ISEC '97, Berlin, Germany, 1997, June 25-28, vol. 3, pp. 392-398.